NUMERICAL SIMULATION OF THE COMBUSTION PROCESSES IN CYLINDRICAL CHAMBERS

Cristiano V. da Silva
Mechanical Engineering Graduate Program - Federal University of Rio Grande do Sul.
Rua Sarmento Leite, 425, 90050-170 - Porto Alegre, RS, Brazil
crisvitor007@yahoo.com.br

Horácio A. Vielmo
Mechanical Engineering Department - Federal University of Rio Grande do Sul.
Rua Sarmento Leite, 425, 90050-170 - Porto Alegre, RS, Brazil.
vielmoh@mecanica.ufrgs.br

Abstract. *This study presets the results of a numerical simulation of the combustion processes of cylindrical chamber with axial symmetry, taking into account two configurations. In the first, the chamber is thermally isolated, whereas in the second, the chamber is immersed in water. For both configurations, two situations are solved: one with a combustion process in stoichiometric relations, and the other with air excess. Simulation is carried out with non-staged combustion process, without pre-mixture. The oxidant and the fuel are injected by a burner. It is assumed that fuel enters through central annular orifices, and the oxidant by an annular duct, external to these orifices, on the same plan. In these simulations, atmospheric air and natural gas are used. The equations of mass, energy, momentum and chemical species conservation are solved. The* $k-\varepsilon$ *turbulence model was applied, and the combustion process is described by the SCRS – Simple Chemically-Reacting Systems. The solution of the equations uses the Finite Volume Method. The results of the mathematical modeling allow the determination of the profile of the combustion zone, the distribution of the concentration of chemical species (fuel and oxygen), and also the velocity fields. Temperature profile is vary important for the prediction of performance of the combustion chamber, as well as to optimize it. The validations of the results were made by comparison with experimental data obtained in the literature, showing good agreement.*

Keywords. *Combustion, Cylindrical Chambers,* $k-\varepsilon$*, SCRS, Finite Volumes.*

1. Introduction

Combustion reactions are present in many industrial processes for the manufacture of products, and also in the direct generation of thermal, electrical, or mechanical energy. In many industrial processes, such as drying of ceramic material, molding of polymers, metal casting, thermal treatments of metal parts, incineration, glass production and molding, and even in food manufacturing, some kind of fuel is burned. Therefore, a better modeling of this phenomenon can directly influence the efficiency of production. During the last twenty-five years, a significant part of these efforts aimed mainly at the development of multidimensional mathematical models for different equipment, such as boilers, reactors, steam generators, and burners. These models serve as tools that reproduce physical experiments through equivalent numerical experiments. The technology of the combustion model can have many forms, but few have the capacity to realistically represent combustion processes. Eaton et al. (1999) presented a revision of approximate models of combustion processes that are capable of simulating these phenomena. The presented models are essentially based on equations of mass, of energy, of chemical species, and of momentum conservation coupled to turbulence models of the $k-\varepsilon$ type (Launder and Spalding, 1972; Launder and Sharma, 1974), combustion models based on the laws of Arrhenius (Kuo, 1986; Fluent, 1997), models of Magnussen – EBU – Eddy Breakup (Magnussen and Hjertager, 1976), and models of heat transfer by radiation of the RTE type – "Radiative Transfer Equation" (Özisik, 1985; Viskanta and Meguç, 1987; Carvalho et al., 1991).

Isnard and Gomes (1998) presented a numerical studies on the formation of NOx in combustion processes by natural gas in cylindrical chambers. The main objective of that study was to investigate the performance of a model based on the formulation in Finite Volumes, which included equations of Navier-Stokes and the $k-\varepsilon$ turbulence model, in addition to energy and chemical species conservation equations, for the estimation of the formation of NOx in industrial combustion processes using natural gas. The generalized model of finite rates of chemical reactions of Arrhenius and Magnussen (Kuo, 1986; Fluent, 1997) was used for the calculation of combustion, and the model DTRM – Discrete Transfer Radiation Model (Carvalho et al., 1991; Fluent, 1997), to calculate of heat transfer by radiation. The determination of NOx formation was made using Zeldovich's mechanisms (Zeldovich et al., 1947). Isnard and Gomes (2000) developed a numerical investigation simulating combustion processes by natural gas in a cylindrical chamber in order to quantify the efficiency of the model by comparison to experimental data. The model used in the present study is similar to the method employed by Isnard and Gomes (1998).

Gorner and Zinzer (1990) simulated a combustion process with multiple burners, and obtained good agreement between numerical and experimental results. Nieckele et al. (2001) performed a numerical analysis involving combustion processes in a cylindrical chamber using the Fluent, where experimental data were evaluated. Nieckele et al. (2002) developed a numerical study on the same geometry used in latter study, using the generalized model of finite rates for the calculation of the chemical reactions (Arrhenius and Magnussen equations). They analyzed two situations for the combustion process: in the first, a single global reaction was used to estimate fuel burning, whereas in the second situation, a two steps reaction was considered. The obtained results were compared to experimental data, and a

good agreement was found. The two steps reaction simulation showed the best results, which were very similar to the experimental data.

In a numerical and experimental study, Magel et al. (1996) investigated the combustion process of natural gas in an cylindrical chamber with axial symmetry combustion chamber with a single burner placed on the symmetry line of the chamber. They obtained the profiles of temperature, oxygen, carbon monoxide, and carbon dioxide concentrations for several positions within the combustion chamber.

The present study presents a numerical simulation of the combustion process of a mixture of air and fuel inside a cylindrical chamber using a model SCRS – Simple Chemically-Reacting Systems (Spalding, 1979). The main objective was to analyze the behavior of the combustion process of natural gas in order to guide the modeling of this process, which may help the design of industrial equipment, such as ovens and steam generators, as well as to verify the efficiency of the SCRS model.

2. Mathematical formulation

In the present study, it is considered that the combustion process occurs instantaneously, and that thermal exchanges have already reached a steady state. Knowing that heat is transferred from the hot gases derived from combustion to the exterior of the chamber, this study initially focused on the analysis of the behavior of the process as to heat transfer, to the concentrations of the components of the mixture, and to the characteristics of the flame and of the outflow inside the combustion chamber. Due to the chamber geometry, the problem is to calculate the distribution of temperatures, of concentrations, and also the velocity field. Mean equations in time were adopted, and the model $k-\varepsilon$ simulates the turbulence in the outflow by the calculation of a turbulent viscosity μ_t, an outflow property. In mathematical terms, this requires the solution of the equations of mass and momentum conservation (Equations of Navier-Stokes), conservation of turbulent kinetic energy and its dissipation (Model $k-\varepsilon$) and conservation of energy and of chemical species (Combustion Model SCRS).

2.1. Movement equations

2.1.1. Mass conservation

$$\frac{\partial}{\partial x}\left(\rho\bar{u}\right)+\frac{\partial}{\partial r}\left(\rho\bar{v}\right)+\frac{\rho\bar{v}}{r}=0, \tag{1}$$

where, $\bar{u}$ and $\bar{v}$ are the mean velocities in the axial and radial directions, ρ is the density, and x and r are the axial and radial coordinates, respectively.

2.1.2. Conservation of axial momentum ($\bar{u}$)

$$\bar{u}\frac{\partial}{\partial x}\left(\rho\bar{u}\right)+\bar{v}\frac{\partial}{\partial r}\left(\rho\bar{u}\right)=-\frac{\partial p^*}{\partial x}+\vec{\nabla}\bullet\left(\left(\mu+\mu_t\right)\vec{\nabla}\bar{u}\right)+\frac{\partial}{\partial x}\left(\mu_t\frac{\partial\bar{u}}{\partial x}\right)+\frac{1}{r}\frac{\partial}{\partial r}\left(r\mu_t\frac{\partial\bar{v}}{\partial x}\right), \tag{2}$$

where, μ represents absolute viscosity; μ_t represents turbulent viscosity, defined as $\mu_t=C_\mu\rho k^2/\varepsilon$; $p^*=\bar{p}-(2/3)k$ is the modified pressure, C_μ is an empirical constant, $\bar{p}$ is the mean pressure, k is the turbulent kinetic energy, and ε its dissipation.

2.1.3. Conservation of radial momentum ($\bar{v}$)

$$\bar{u}\frac{\partial}{\partial x}\left(\rho\bar{v}\right)+\bar{v}\frac{\partial}{\partial r}\left(\rho\bar{v}\right)=-\frac{\partial p^*}{\partial r}+\vec{\nabla}\bullet\left(\left(\mu+\mu_t\right)\vec{\nabla}\bar{v}\right)+\frac{\partial}{\partial x}\left(r\mu_t\frac{\partial\bar{u}}{\partial r}\right)+\frac{1}{r}\frac{\partial}{\partial r}\left(r\mu_t\frac{\partial\bar{v}}{\partial r}\right)-\frac{\left(\mu+\mu_t\right)\bar{v}}{r^2}+\frac{\rho\bar{w}^2}{r}, \tag{3}$$

where, $\bar{w}$ in the mean tangential velocity due to the presence of a stator at the air entrance region.

2.1.4. Conservation of angular momentum ($r\bar{w}$)

$$\bar{u}\frac{\partial}{\partial x}\left(\rho r\bar{w}\right)+\bar{v}\frac{\partial}{\partial r}\left(\rho r\bar{w}\right)=\vec{\nabla}\bullet\left(\left(\mu+\mu_t\right)\vec{\nabla}r\bar{w}\right)-\frac{2\left(\mu+\mu_t\right)}{r}\frac{\partial}{\partial r}\left(r\bar{w}\right). \tag{4}$$

2.2. Turbulence model $k-\varepsilon$

2.2.1. Conservation of turbulent kinetic energy k and its dissipation ε

$$\bar{u}\frac{\partial}{\partial x}(\rho k)+\bar{v}\frac{\partial}{\partial r}(\rho k)=\vec{\nabla}\bullet\left(\left(\mu+\frac{\mu_t}{\sigma_k}\right)\vec{\nabla}k\right)+P_k-\rho\varepsilon\,, \tag{5}$$

and

$$\bar{u}\frac{\partial}{\partial x}(\rho\varepsilon)+\bar{v}\frac{\partial}{\partial r}(\rho\varepsilon)=\vec{\nabla}\bullet\left(\left(\mu+\frac{\mu_t}{\sigma_\varepsilon}\right)\vec{\nabla}\varepsilon\right)+C_{1,\varepsilon}\frac{\varepsilon}{k}P_k-C_{2,\varepsilon}\frac{\varepsilon^2}{k}\,, \tag{6}$$

where, $C_{1,\varepsilon}$ and $C_{2,\varepsilon}$ are empirical constants, σ_k e σ_ε represent the numbers of Prandtl for turbulent kinetic energy and its dissipation, respectively, and P_k represents the production or dissipation of turbulent kinetic energy, defined as,

$$P_k=\mu_t\left(2\left(\frac{\partial\bar{u}}{\partial x}\right)^2+\left(\frac{\partial\bar{u}}{\partial r}+\frac{\partial\bar{v}}{\partial x}\right)^2+2\left(\frac{\partial\bar{v}}{\partial r}\right)^2+2\left(\frac{\bar{v}}{r}\right)^2\right). \tag{7}$$

2.3. Combustion model SCRS

2.3.1. Conservation of chemical species

The model of simplified chemical reaction assumes that the combustion reaction occurs instantaneously, and that oxygen and fuel do not co-exist. Only three chemical species are present in the mixture – oxygen, fuel, and products –, and therefore equations of conservation are needed for each of the species. However, knowing that in turbulent outflows the diffusion of chemical species due to turbulence is dominant over molecular diffusion, it is assumed with good approximation that the coefficients of mass diffusivity of these chemical species are identical (Spalding, 1979). Therefore, only one equation of conservation needs to solved, and as SCRS assumes that fuel and oxidant consist of a single chemical reaction, and as the result of this reaction is assumed as products, with the introduction of an auxiliary calculation variable, f_{fx}, we have the following equation of conservation of chemical species

$$\bar{u}\frac{\partial}{\partial x}\left(\rho\overline{f_{fx}}\right)+\bar{v}\frac{\partial}{\partial r}\left(\rho\overline{f_{fx}}\right)=\vec{\nabla}\bullet\left(\rho\left(D+\frac{\mu_t}{\sigma_t}\right)\vec{\nabla}\overline{f_{fx}}\right), \tag{8}$$

where, D is mass diffusivity, and σ_t is the Prandtl turbulent number. The variable f_{fx} is locally treated in the domain of calculation as $f_{fx}=f_{comb}-(f_{ox}/s)$, where, f_{comb} and f_{ox} are the fuel and oxygen fractions, respectively, and s is the stoichiometric relation between its masses. Therefore, by analyzing of the signal of f_{fx}, it is possible to identify the fuel-rich regions and the oxygen-rich region. When f_{fx} is higher than zero, the region is rich in fuel, whereas when f_{fx} is lower than zero the region is rich in oxygen. The model illustrates this fact

$$f_{fx}>0\rightarrow\left\{\begin{matrix}f_{ox}=0\\f_{comb}=f_{fx}\end{matrix}\right\}, \tag{9}$$

and

$$f_{fx}<0\rightarrow\left\{\begin{matrix}f_{comb}=0\\f_{ox}=-sf_{fx}\end{matrix}\right\}. \tag{10}$$

2.3.2. Conservation of energy

For the transport of energy due to the outflow of fluids inside the chamber, ignoring the part referring to the transport of energy due to the diffusion of each species, we have

$$\bar{u}\frac{\partial}{\partial x}\left(\rho\left(\int c_pT+H^{comb}f_{comb}\right)\right)+\bar{v}\frac{\partial}{\partial r}\left(\rho\left(\int c_pT+H^{comb}f_{comb}\right)\right)=\vec{\nabla}\cdot\left(\left(\frac{\kappa}{c_p}+\frac{\mu_t}{\sigma_t}\right)\vec{\nabla}\left(\int c_pT+H^{comb}f_{comb}\right)\right), \tag{11}$$

where, c_p is the specific heat of the mixture, defined as, $c_p = \sum_{\alpha} f_\alpha c_{p,\alpha}$, with $c_{p,\alpha}$ and f_α as the specific heat and the mass fraction of the α-esimal chemical species, T is temperature, H^{comb} is the enthalpy of combustion, and κ the thermal conductivity of the mixture. The variables preserved in Eq. (11) represent the energy transported by the fluid, and can be added as a single variable. The mean enthalpy of the mixture is defined as $\overline{h} = \int c_p T + H^{comb} f_{comb}$.

Completing the model, it is possible to determine the density of the mixture by the equation of the state of the ideal gases (Spalding, 1979; Fluent, 1997), $\rho = p\overline{MM}\left(\overline{R}T\right)^{-1}$, where p is the pressure of operation of the chamber, which in this equation is assumed as 1 atm (Spalding, 1979), $\overline{MM}$ is the molecular mass of the mixture, and $\overline{R}$ is the universal constant of gases.

All equations presented until now are only valid for the turbulent core, where $\mu_t >> \mu$. Close to the solid walls, where $\mu_t << \mu$, the law of the wall recommended by Freire et al. (2002) is used. The law of the wall is obtained by assuming turbulent equilibrium in the regions next to solid surfaces. It must be applied to the region between the wall and the first nodal point of the simulation. This law consists in assigning a logarithm velocity profile to the completely turbulent region and a linear profile to the laminar sub-layer. Therefore, for $y^+ \le 11.5 \rightarrow u^+ = y^+$, and $y^+ > 11.5 \rightarrow u^+ = (1/\mathrm{A})\ln(y^+) + \Psi$, where $y^+ = y\left(\rho C_\mu^{\frac{1}{4}} k^{\frac{1}{2}} \mu^{-1}\right)$, is the normal non-dimensional distance to the wall, $u^+ = \overline{u}/u^*$, is the non-dimensional velocity, $u^* = \sqrt{\tau_w/\rho}$, is the velocity of friction, being τ_w the shearing tension on the wall, and y the normal distance to the wall. According to Nikuradse (1933), the values of the constants A and Ψ, which appear in the u^+ equation, are 0.4 and 5.5, respectively.

According to the hypothesis of equlibrium between the production and the destruction of turbulent kinetic energy, also considering that the shearing stress on the wall is approximately constant in this region, the normal gradient of kinetic energy on the walls is null. The dissipation of turbulent kinetic energy is determined by the expression, $\varepsilon = C_\mu^{3/4} k^{3/2} \left(\mathrm{A}y\right)^{-1}$.

3. Physical problem

The analyzed geometry is based on the experimental apparatus of Magel et al. (1996). A cylindrical combustion chamber measuring 1.7 m length and 50 cm diameter, as shown in Fig. (1), is considered. This combustion chamber is fed with natural gas (GN) through the injection nozzle of the burner placed on its axial symmetry line. The burner supplies the combustion chamber with the necessary quantities of air and fuel. As natural gas consists of 90% methane (CH_4), it was used as the single component of fuel. In Eq. (12), considering the air consisting only of oxygen and nitrogen, the chemical reaction of stoichiometric combustion of methane can be observed,

$$CH_4^{(16)} + 2O_2^{(32)} + 2(3.76)N_2^{(28)} \rightarrow CO_2^{(44)} + 2H_2O^{(18)} + 2(3.76)N_2^{(28)}. \quad (12)$$

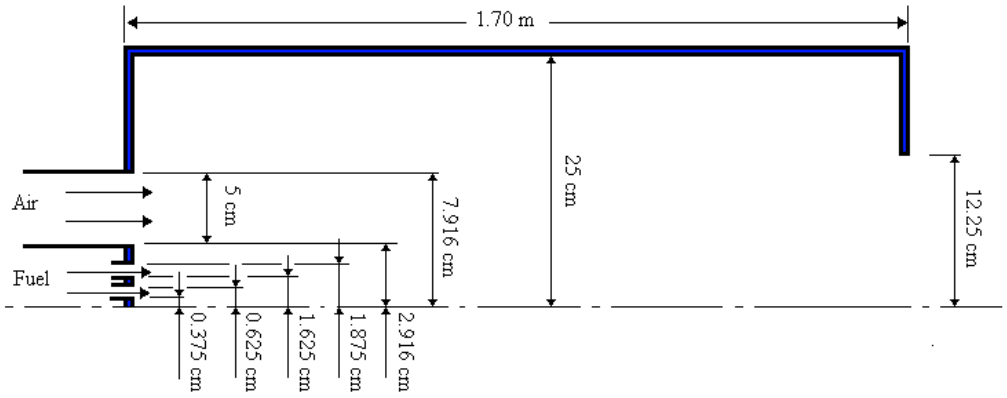

Figure 1. Geometry of the chamber.

It is assumed that the fuel enters through central annular openings, and that the oxidant enters through an annular duct, external to these openings, on the same plan, as shown in Fig. (1).

Taking into consideration the axial symmetry, the calculation domain is assumed as being merely an angular fraction, which is representative of the chamber (1 radian). It is also assumed that the nitrogen present in the reaction remains inert. The mass composition of dry air is 23.25% oxygen, and 76.85% nitrogen. Hence, dividing the oxygen/fuel ratio, which is 4:1, by the quantity of oxygen present in dry air, it is found that 17.24 kg of this air is

needed to oxidize 1 kg methane. It is also considered that the main component of the products is nitrogen, as it is present in a higher proportion. Therefore, before combustion, the mixture consists of methane, oxygen and nitrogen. For modeling, it is assumed that both fuel and air are initially injected at constant velocity and temperature. The radiation heat transfer is not being taken into consideration, and the buoyancy forces due to variation in density are ignored, as advection is dominant. The additional terms due turbulence are not considered at conservation of angular momentum equation.

4. Studied cases

Two cases were studied. In case I, a boundary condition of null thermal flow (adiabatic walls) was applied to the external walls of the chamber. In case II, it was considered that the combustion chamber was immersed in water, applying to its walls a boundary condition of the third kind (coefficient of heat transfer $h_{\inf}$ and constant $T_{\inf}$ temperatures). In this case, it was also assumed that the chamber walls are made of steel and are 5-mm thick, and which resistance to diffusion is included in $h_{\inf}$.

In both cases, the air/fuel ratios used in the analysis of the combustion chamber were 17.24:1 (stoichiometric combustion), and 25.85:1 (air excess of 50%). The velocities of air injection were 20 m/s and 30 m/s both for cases I and II. Due to the presence of a stator in the burner, the tangential entry velocity equal to 20% of the axial entry velocity, the power of the burner of 150 kW/rd, and the entry temperature of air and fuel entry of 323.15 K were assumed in order to compare the results.

5. Thermophysical properties

The constants present in the equation, and the thermophysical properties of the gases involved were taken from several references, and are presented in Tab. (1). It is assumed that all thermophysical properties present in the problem remain constant for each substance, except for the specific heat of the gases (CH_4, O_2 and N_2). Table (2) shows the specific heat values at constant pressure as a function of temperature. The specific heat of the mixture was obtained from the weighed mean from the mass fractions of each species. The thermophysical properties of the air are used for the mixture, as it is proportionally present in higher quantity.

Table 1. Thermophysical properties used in the solution of the problem (several references).

Property	Magnitude	Properties	Magnitude
σ_t (-)	0.9	$\overline{MM}_{CH_4}$ (kg/kmol)	16
$c_{p,Fe}$ (J/kgK)	434	$\overline{MM}_{O_2}$ (kg/kmol)	32
κ_{Fe} (W/mK)	60.5	$\overline{MM}_{N_2}$ (kg/kmol)	28
κ (W/mK)	64.7×10^{-3}	D (m^2/s)	1.19×10^{-4}
$\overline{R}$ (kJ/kmolK)	8.3145	μ (Ns/m^2)	4.23×10^{-5}
H^{comb} (J/kg)	5.0×10^{7}	σ_ε (-)	1.3
$C_{2,\varepsilon}$ (-)	1.92	σ_k (-)	1.0
$C_{1,\varepsilon}$ (-)	1.44	C_μ (-)	0.09

Table 2. Specific heat at constant pressure as a function of temperature (Nieckele et al., 2001).

Temperature (K)	$c_{p,comb}$ (J/kgK)	$c_{p,ox}$ (J/kgK)	c_{p,N_2} (J/kgK)
300	2226	914	1045
600	3256	1005	1075
1000	4475	1084	1164
1500	5408	1360	1239
2000	5904	1175	1283
2500	6165	1215	1314

6. Boundary conditions

Except for the thermal problem, the boundary conditions are the same for both studied cases.

A non-sleep (zero velocity) and impermeability condition was used on the wall. In the symmetry axis, the radial gradient of all velocities was assumed as null. The radial component of velocity is null in this axis. The exit condition for all variables was null diffusive flow, being the axial component of the velocity downstream of the chamber exit corrected for one factor in order to conserve mass and to avoid counter flows.

In the entry section, a uniform outflow in the axial direction, with a uniform concentration profile in each entry region was assumed. The turbulent kinetic energy was assumed as $k = 5.0x10^{-3}(\bar{u})^2$. The rate of turbulent kinetic energy dissipation was specified as $\varepsilon = 1.0x10^{-1}(k)^2$.

7. Numerical method

The numerical solution of the conservation equation was numerically obtained by the Finite Volume Method, as described by Patankar (1980). The Power-Law distribution was selected to evaluate the flows on the sides of the control volumes. The pressure-velocity coupling was solved by the SIMPLE algorithm. The obtained algebraic equation system was solved by TDMA, using the technique of correction in block, except for turbulent kinetic energy and its dissipation.

Due to the strong coupling among the equations and to the non-linearities, sub-relaxations equal to 0.1 are employed in all equations in order to avoid divergence of solutions. Mesh-independence tests were performed, obtaining 100 volumes in the axial directions, and 100 volumes in the radial direction. This mesh allowed a good behavior between the quality of solution and the computational time. Linearization and discretization in Finite Differences of the source terms of the conservation equations were performed when necessary. In case II, the boundary condition of the third kind was incorporated in the source terms of boundary volumes.

8. Validation of the model

In order to validate the modeling of the present study, a situation implementing boundary and entry conditions similar to those used in the study of Nieckele et al. (2001), comparing their results with the experimental results of Magel et al. (1996), was solved. The geometry analyzed in the present situation consists of a cylindrical oven with adiabatic walls with a diameter of 50 cm and a length of 1.7 m. The fuel is injected by a central 6-cm-diameter opening, and air by an adjacent ring with an internal length of 5 cm. Air was injected at a temperature of 323.15 K, with a density of 1.2 kg/m^3, and a discharge of 0.186 kg/s, corresponding to a velocity of 36.3 m/s. Methane gas was injected at a temperature of 313.15 K, with a density of 0.646 kg/m^3. Fuel discharge was dispensed at 0.0125 kg/s, corresponding to a velocity of 27.69 m/s. The diameter of the chamber exit orifice is 25 cm.

Figure (2) shows the temperature profiles of hot gases on the symmetry line of the combustion chamber, referring to the experimental results of Magel et al. (1996), as well as to the numerical simulation solved by the combustion model of Arrhenius-Magnussen by Nieckele et al. (2001), and also to the solution using the present modeling (SCRS combustion model).

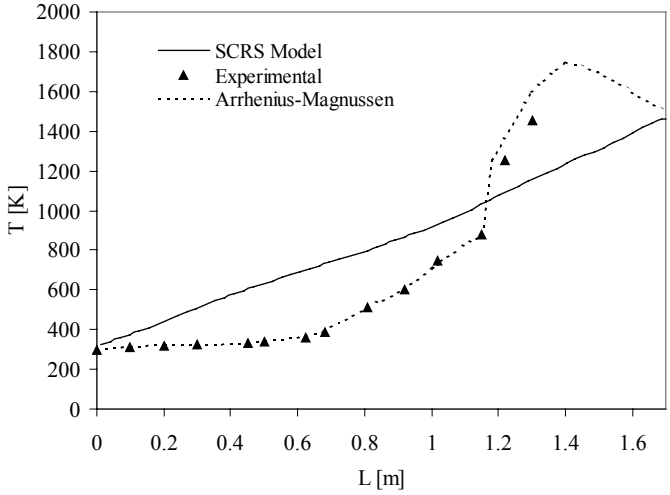

Figure 2. Gas temperature on the symmetry line of the combustion chamber.

We can observe in Fig. (2) that the temperature profile of the gases obtained by the SCRS model follows the general trend, but in a more linear fashion. It also presents virtually the same temperature at the exit region.

9. Analysis of the results

Figure (3) shows the results for the combustion process occurring under the condition of stoichiometry for case I, after the process had reached the steady state. Figure (3-a) presents the distribution of oxygen mass fraction inside the chamber. In this figure, we can distinctly observe the region occupied by the chamber, which is the central area in light blue. We can also observe that, in the top left area of the chamber, which is the area into which the air is being injected, higher concentrations of oxygen predominate, and there are no signs of combustion.

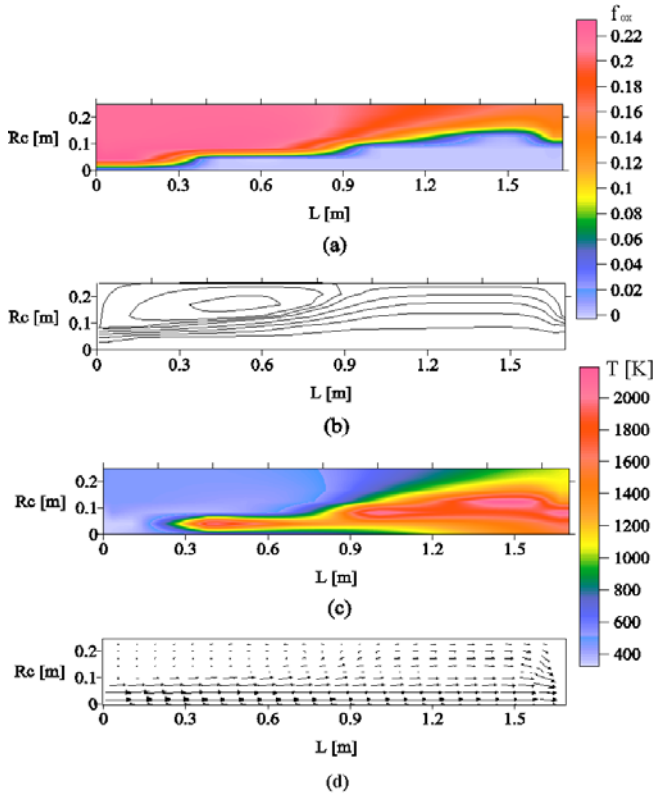

Figure 3. Behavior of the combustion process for case I – Stoichiometric combustion: (a) Oxygen mass fraction, (b) Stream function, (c) Temperature distribution, (d) Velocity vectors.

Figure (3-b) shows the isolines of the stream function. In this figure, we can observe the existence of a secondary outflow in the shape of a large recirculation situated on the left top area. This occurs due to the high velocity of air and fuel injection by the burner located immediately below this recirculation, at the chamber entry. It is formed by a low-pressure region on the left top corner, determining an inversion of the flow, and forming this vortex, which is maintained by the shearing stress between the main outflow and this secondary outflow.

Figure (3-c) presents the distribution of the temperature of the gases inside the combustion chamber. This figure shows that there are very distinct regions. In the central region, next to the central line, we can clearly identify a region with lower temperatures, corresponding to the cold injection of the high-velocity entry. There are also two regions in the central part, located on the right side of the chamber, where there are significant increases in gas temperature. This phenomenon is associated to the fuel not yet burned, which temperature is higher than at the entry, as a reaction with the oxygen still present, promoting a new burning stage in the combustion process, and thus reaching higher temperatures inside the chamber.

Figure (3-d) shows the behavior of the velocity vectors as a function of the presence of air and fuel flows. By comparing velocity vector scales, the highest velocities inside the chamber are of approximately 62 m/s, and the lowest about 4 m/s. Therefore, analyzing the vectors, we find that the highest velocities are located near the center of the combustion chamber (symmetry line), and at the exit area, as well as that the lowest velocities are present within re-circulation, caused by flow inversion, and close to the walls.

Figure (4) shows temperature profiles for both situations studied in case I. We can see in the Fig. (4) that the temperature profiles have the same characteristics, with almost the same temperature peaks, but in different positions of the radial direction. The temperature difference presented among the profiles happens due to air excess. In the case of stoichiometric combustion, the temperature of the exiting gas is lower for the case of air excess from the peak to the symmetry line, whereas the opposite happens from the peak to the upper part of the exit orifice. As this excess of relatively cold air occurs mostly around the external ring, the temperature in this region is lower. On the contrary, the region near the symmetry axis is highly heated because of the higher availability of air and natural gas for combustion.

Figure (5) presents the profiles of oxygen concentration in the gases at the exit for the same situations presented in Fig. (4). It is observed that the profile of oxygen concentration for the situation of stoichiometric combustion indicates lower concentration than in the case of combustion with air excess, as expected. An opposite analogy can be applied to the fuel concentration at the exit, as shown in Fig. (6). The highest the concentration of oxygen, the higher are the chances of a reaction between oxygen and fuel. These figures also show that temperature peaks observed in Fig. (4) occur precisely on the boundary where there is still oxygen available for combustion. In Fig. (6), due to the higher

amount of air injected when there is a condition of air excess, a lower amount of fuel is present in the gases at the exit, improving the burning efficiency of the process. Associating the amount of fuel leaving the chamber in the combustion gases to the amount of injected fuel, an analysis of the burning efficiency of the process is obtained. This analysis resulted in a burning efficiency of 71.6% for the case of stoichiometric combustion, and 86.8% for the condition of air excess.

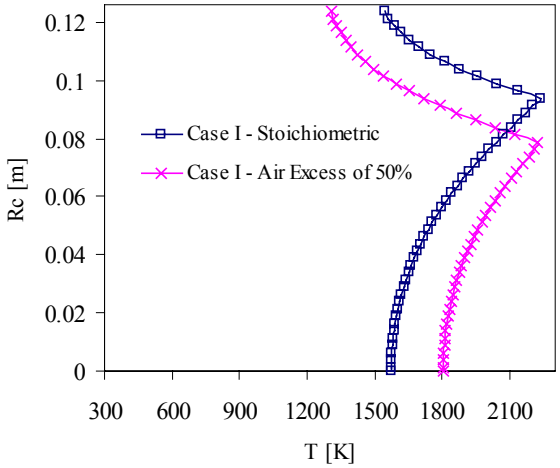

Figure 4. Temperature profile of the gases at the exit of the combustion chamber in case I.

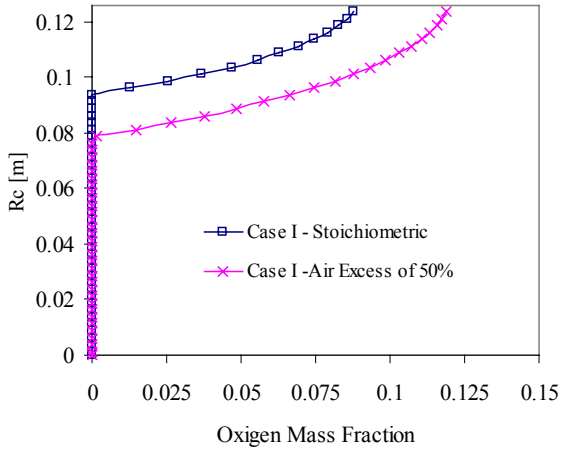

Figure 5. Oxygen concentration in the gases at the exit of the combustion chamber for case I.

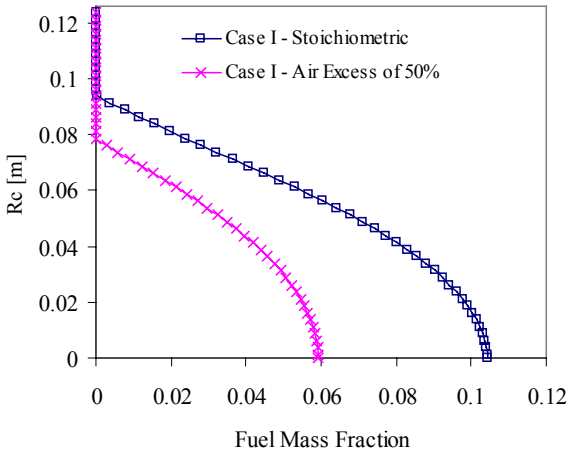

Figure 6. Fuel concentration in the gases at the exit of the combustion chamber for case I.

In order to check the influence of the boundary condition on the temperature of the exiting gases, Figs. (7) and (8) illustrate the comparison of temperature profiles of these gases in cases I, and II in a condition of stoichiometric combustion. In Fig. (7), we can observe the influence of thermal exchange with the external environment on the

temperature gases exiting the combustion chamber. Except for the regions near the walls, results are very similar. The difference is related to the existence of a convective heat flow to the external part of the chamber, cooling the gases in this region, which did not happen in case I. Fig. (8) shows temperature distribution at the exit of the combustion chamber. We can observe in this figure that the temperature of the gases is virtually the same from the symmetry line up to the temperature peak (Rc ≈ 0.09 m). For case II, due to the thermal exchanges with the external environment, temperature profile of the gases is lower from this point to the upper part of the exit orifice (Rc = 0.125 m).

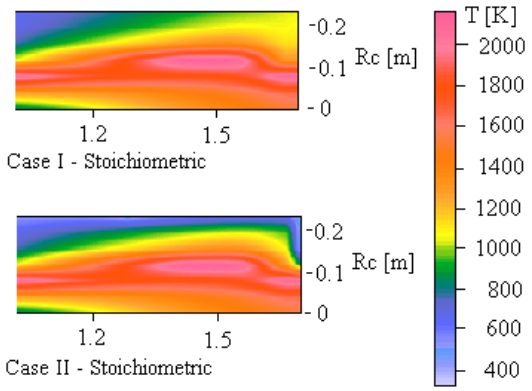

Figure 7. Temperature distribution in the combustion chamber for cases I and II under the condition of stoichiometry.

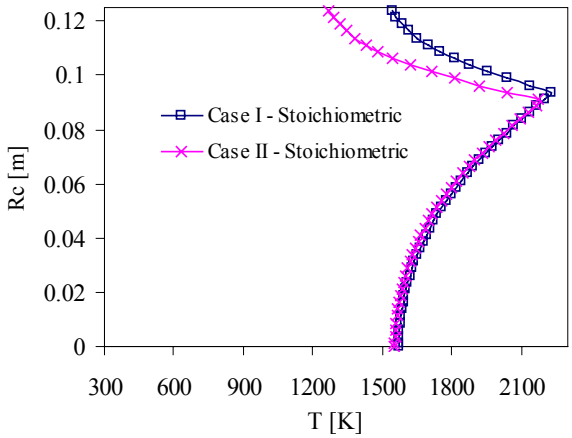

Figure 8. Temperature profile of the gases exiting the combustion chamber for cases I and II under the condition of stoichiometry.

10. Conclusions

Based on these investigations of the combustion process, the following conclusions can be drawn:

1- As expected, the injection of air excess during the combustion process is critical to ensure better efficiency of fuel burning.
2- The conditions of air and fuel entry, as well as the proportions between these two substances, and the velocity of injection, have a significant influence on the distribution of temperatures and concentrations during the process.
3- The boundary conditions employed in the energy equation had little influence on the combustion process, as well as on the profiles of temperature and concentration of the exiting gases. Their influence was restricted to a small region very close to the walls.
4- SCRS is able to generate coherent results in terms of general trends, and can be used in rapid investigations.

11. Acknowledgements

The authors thank for the support of CNPq – National Research Council (Brazil) – by granting a doctoral scholarship to the first author.

12. References

Carvalho, M.G., Farias, T. and Fontes, P., 1991. “Predicting radiative heat transfer in absorbing, emitting, and scattering media using the discrete transfer method”, ASME HTD, Vol. 160, pp.17-26.

Eaton, A.M., Smoot, L.D., Hill, S.C. and Eatough, C.N., 1999. “Components, formulations, solutions, evaluations, and application of comprehensive combustion models”, Progress in Energy and Combustion Science, Vol. 25, pp. 387-436.

Fluent (ed.), 1997. “Fluent user’s guide”, Fluent Incorporated, New Hmpshire.

Freire, A.P.S., Menut, P.P.M. and Su, J., 2002. “Turbulência”, Associação Brasileira de Ciências Mecânicas – ABCM, Rio de Janeiro – BR, Vol. 1.

Gorner, K. and Zinzer, W., 1990. “Simulation of industrial combustion systems”, Int. Chem. Eng., Vol. 30, No.4, pp. 607-619.

Isnard, A.A. and Gomes, M.S.P., 1998. “Numerical investigation on the Nox formation in natural gas combustion”, VII Encontro Nacional de Ciências Térmicas, ENCIT98, Rio de Janeiro – RJ.

Isnard, A.A. and Gomes, M.S.P., 2000. “Predicting the NO formation in natural gas combustion”, Congresso Nacional em Engenharia Mecânica, CONEM/2000, Natal – RN.

Kuo, K.K., 1996. “Principles of combustion”, John Wiley & Sons, New York.

Launder, B.E. and Spalding, D.B., 1972. “Mathematical Model of Turbulence”, Academic Press Inc. LTD.

Launder, B.E. and Sharma, B.I., 1974. “Application of the energy-dissipation model of turbulence to the calculation of flow near a spinning disc”, Letters in Heat and Mass Transfer, Vol. 19, pp. 519-524.

Magel, H.C., Schnell, U. and Hein, K.R.G. ,1996. “Modeling of hydrocarbon and nitrogen chemistry in turbulent combustor flows using detailed reactions mechanisms”, 3rd Workshop on Modeling of Chemical Reaction Systems, Heidelberg.

Magnussen B.F. and Hjertager B.H., 1976. “On mathematical models of turbulent combustion with special emphasis on soot formation and combustion. Proceedings of the 16th International Symposium on Combustion, The Combustion Institute, pp. 719–729.

Nieckele, A.O., Naccache, M.F., Gomes, M.S.P., Carneiro, J.E. and Serfaty, R., 2001. “Evaluation of models for combustion processes in a cylindrical furnace”, ASME-IMECE, International Conference of Mechanical Engineering, New York.

Nieckele, A.O., Naccache, M.F., Gomes, M.S.P., Carneiro, J.E. and Serfaty, R., 2002. “Predição da combustão de gás natural em uma fornalha utilizando reação em uma e duas etapas”, CONEM – Congresso Nacional de Engenharia Mecânica – João Pessoa – PB.

Nikuradse, J., 1933. “Strömusgsgesetze in Rauhen Rohren”, Forsch. Arb. Ing. – Ees.

Özisik, M.N., 1985. “Heat Transfer”, 1st edn, McGaw-Hill Book Company, New York.

Patankar, S.V., 1980. “Numerical Heat Transfer and Fluid Flow, Hemisphere”, New York.

Spalding, D.B., 1979. “Combustion and Mass Transfer”, Pergamon Press, Inc., New York.

Viskanta, R. and Meguç, M.P., 1987. “Radiation heat transfer in combustion system”, Progress in Energy and Combustion Vol. 13, pp. 97-160.

Zeldovich, Y.B., Sadovnikov, P.Y. and Frank-Kamentskii, D.A., 1947. “Oxidation of nitrogen in combustion”, Academy of Science of USSR, Moscow.